Conformational Flexibility in Designing Peptides for Immunology: The Molecular Dynamics Approach

Athanassios Stavrakoudis*

Department of Economics, University of Ioannina, 451 10, Ioannina, Greece

Abstract: Computational modeling techniques and computer simulations have become a routine in biological sciences and have gained great attention from researchers. Molecular dynamics simulation is a valuable tool towards an understanding of the complex structure of biological systems, especially in the study of the flexibility of the biological molecules such as peptides or proteins. Peptides play a very important role in human physiology and control many of the processes involved in the immune system response. Designing new and optimal peptide vaccines is one of the hottest challenges of the 21st century science and it brings together researchers from different fields. Molecular dynamics simulations have proven to be a helpful tool assisting laboratory work, saving financial sources and opening possibilities for exploring properties of the molecular systems that are hardly accessible by conventional experimental methods. Present review is dedicated to the recent contributions in applications of molecular dynamics simulations in peptide design for immunological purposes, such as B or T cell epitopes.

Keywords: B cell, T cell, TCR, complement system, computer simulation, MHC, antigen, antibody, antibody-antigen interactions, epitope, molecular dynamics, epitope prediction, vaccine design.

INTRODUCTION

Discovering new effective drugs is one of the biggest scientific challenges of our time. This target has become a field for joint efforts from both industry and academia as well as from both public and private sectors of the society. The completion of the human genome project raised great expectations about drug discovery. However, the elucidation of human genes did not mean that the function of gene's products would be completely understandable. Gene encoded proteins may have extremely different properties: they may be globular or may be not, they may be water soluble or interact with membranes, they may be carriers, enzymes, receptors etc. Furthermore, they undergo numerous post-translation modifications that alter their chemical component. Finally, proteins have one unique characteristic: they are not simple polymers or just a sequence of building blocks but they have 3D configuration that matters a lot in their function. Proteins can also break into small pieces: the peptides. Even though cells can produce peptides, proteolytically derived peptides play a very important role in human physiology by triggering the immune system response and by interacting with various receptors, such as antibodies and TCRs (T cell receptors) after loading to MHC (Major histocompatibility complex) molecules. There is an increasing interest in using peptide or peptide-based drugs [1-3]. Some endogenous peptides have been also used as drug targets [4]. Peptides are even more flexible than proteins in solution (for an example see ref. [5]). However, protein receptors can recognize precisely these highly mobile molecules and form stable complexes. Protein receptors can be flexible as well [6-8]. Targeting these complexes, thus trying to produce peptides that bind better or peptides that antagonize the native binders is the aim of the peptide science.

The task of finding the optimal ligand position within a receptor is called docking [9]. However, in case of peptides and proteins, docking faces another problem: peptide's flexibility [10, 11]. Managing peptide and protein flexibility in docking problems is not a trivial task [10, 11] and computational methods offer a framework to tackle this problem.

Computational methods are extensively applied in biological research and drug discovery [12, 13]. Molecular dynamics computer simulation is a well documented technique to study the structure and function of biomolecules [11-16]. More than three decades have passed since the first publication on computer simulation of BPTI (Bovine Protein Trypsin Inhibitor) molecular dynamics [14]. MD (Molecular dynamics) simulations can contribute to a deeper and more detailed understanding of particle motion as time evolution properties. Experiments may offer a solid background for comparison and validation of results obtained from simulation studies, but there are specific system properties that are hardly accessible through experiments [15]. In cases where specific atomic motions are of interest, MD simulations have a lot to offer [16]. This information is profitable, despite the approximations and limitations [17, 18] caused by the use of force fields [19, 20], because the user can "play" with the parameterization in order to adapt the methodology to a particular problem. In general, MD simulations can be applied in three areas [21]:

1. conformational sampling.
2. studying equilibrium properties and to obtain values of thermodynamic related properties.
3. studying dynamics of a system.

In cases 1 and 2, MC (Monte Carlo) simulations can be used as well, while in case 3 only MD simulations can be

*Address correspondence to this author at the Department of Economics, University of Ioannina, 451 10, Ioannina, Greece; Tel: +30 265 100 5935; Fax: +30 265 100 5092; E-mail: astavrak@cc.uoi.gr

1573-4099/10 $55.00+.00

used. MD simulations have been used extensively for assessment of peptide design, such as epitope prediction [22] or vaccine design [23-27], enzyme mimicking peptides [28-31] or folded peptides [32-36]. The application of MD simulations has been recently connected with patient-specific decisions-makings [25]. In the current review, I will try to highlight some important case studies of peptide/protein complexes related to immune system. There are obviously other than peptide/protein complexes (like protein/protein) that are of interest in immunological research. For an excellent review of application of MD simulations in this field the reader might see ref. [26]. All the contributions reviewed here were carried out (at least partly) with application of MD simulations.

MOLECULAR DYNAMICS SIMULATIONS

Classical molecular dynamics simulation is certainly an approximation of a physical system such as a peptide or protein. From an experimentalist point of view, it is fiction aspiring to reproduce reality. While this is true, it must be noted that carefully performed MD simulations can add significant value in biomolecules of scientific interest. Despite all the inherent approximations, MD simulations can perform very well when certain assumptions are met. In general, MD solves the Newton's equation of motion of a system:

$$m\frac{d^2\vec{r}_i}{dt^2} = \vec{F}_i = -\vec{\nabla}_i U(\vec{R}) \tag{1}$$

A quite general form of a force field is (for a detailed description of force fields see ref. [19, 20]):

$$\begin{aligned} E = & \sum_{bonds} k_b(b-b_0)^2 + \sum_{angles} k_b(b-b_0)^2 \\ & + \sum_{torsions} k_\varphi[(1-\cos(n\varphi)] + \sum_{imporers} k_\omega(\omega-\omega_0)^2 \\ & + \sum_i \sum_{j\neq i} 4\varepsilon\left[\left(\frac{\sigma_{ij}}{r_{ij}}\right)^{12} - \left(\frac{\sigma_{ij}}{r_{ij}}\right)^{6}\right] \\ & + \sum_i \sum_{j\neq i} \frac{q_i q_j}{D r_{ij}} \end{aligned} \tag{2}$$

where the last two double sum terms stand for the van der Waals and electrostatic interactions of the system. Specific implementations of particular MD packages may have altered or extra terms, such as hydrogen bond potentials.

Commonly used software packages in biomolecular simulation are AMBER [37] CHARMM [38] NAMD [39] GROMOS [40] and GROMACS [41]. GROMACS and NAMD have gained considerable popularity during latest years, mainly because they are freely available for academic users. These simulation packages come along with analysis tools, which can be very time consuming sometimes. There is also a continuous interest in developing MD analysis tools that facilitate certain post-simulation tasks [42, 43]. It is worth noting that storing and managing MD results is not a trivial task. Full solvated MD trajectories can occupy several Gbytes of disk space and a considerable amount of physical memory is needed to perform analysis tasks. Current evolution in desktop computers power has contributed a lot to the application of MD simulations.

It is possible from MD simulation results to calculate macroscopic properties as weighted averages:

$$\langle A \rangle = \sum_i \rho(\Gamma_i) A(\Gamma_i) \tag{3}$$

Which correspond to the continuous limit of:

$$\langle A \rangle = \int \rho\Gamma(A)(\Gamma) d\Gamma \tag{4}$$

Current trend in MD simulations of biomolecules is to include solvent representation in the system and to avoid vacuum simulations. Continuum models have been used extensively in MD simulations [44-46]. However, several published works have recognized the importance of explicit water inclusion in the simulation setup.

There is plenty of topics concerning the details of MD simulations. Three of them are briefly presented: a) calculating free energy of binding, b) calculating entropy and c) accounting the convergence of MD trajectories.

FREE ENERGY CALCULATIONS

MD simulations can be used to extract thermodynamic quantities such as ΔG of ligand binding [47-50]. The most commonly used technique, namely MM-PBSA (Molecular Mechanics Poisson-Boltzmann Surface Area) [47, 51-53] is highlighted here (for a detailed review of other techniques see ref. [47]). If two molecules A and B associate and form a complex then the free energy of binding can be calculated as:

$$\Delta G_{bind} = G_{tot}(complex) - G_{tot}(A) - G_{tot}(B) \tag{5}$$

where G_{tot} of each species is:

$$G_{tot} = E_{MM} + G_{PBSA} - TS_{MM} \tag{6}$$

where E_{MM} is the total molecular mechanics energy of a molecular system; G_{PBSA} is the calculated free energy of solvation; T is the absolute temperature and S_{MM} is the entropy. The E_{MM} term can be calculated with the use of a force field and the coordinates of a molecular system. The solvation term G_{PBSA} is split into two terms: the electrostatic contribution and the non-polar solvation:

$$G_{PBSA} = G_{PB} + G_{np} \tag{7}$$

The non-polar solvation term (G_{np}) can be calculated with the solvent accessible surface area model [54], while the electrostatic term corresponds to the Poisson-Boltzmann energy term which can be calculated with software such as APBS [55]. The entropy term is the most difficult to compute [56], although it is not absolutely necessary doing that when only relative binding affinities are to be computed [49] and it can be estimated by quasi-harmonic analysis [56-58] of the trajectory or by using normal mode analysis [59].

ENTROPY CALCULATIONS

Entropy plays an important role in protein/protein association and thus in antigen recognition [59, 60]. Conformational changes have been observed in both antibodies and antigens after binding [60]. MD simulations

offer a very good framework to study these changes from entropic perspective for both solvent and solute molecules [57]. Recently, Hsu *et al*. [60] proposed a heuristic formula based on the covariance matrix of atom-positional fluctuations to assess the configurational entropy. The simultaneous evaluation of different interaction modes through a decomposition approach is only feasible with the knowledge of the atomic trajectory of the system. The configurational entropy analysis in terms of combined trajectories provides very good estimations of thermodynamic properties of biomolecules given that sufficient sampling of conformational space has been performed. Details of calculations can be found in ref. [60], here is a quick presentation of the method:

Schliter's formulation [61] can be used for the calculation of the configurational entropy (S):

$$S_{true} < S = \frac{1}{2} k_B \ln \det \left[1 + \frac{k_B T e^2}{\hbar^2} \mathbf{M}\sigma \right] \quad (8)$$

where S is an upper estimation of the true entropy (S_{true}), k_B is the Boltzmann's constant, T is the absolute temperature (in which the system was simulated), e is Euler's number, $\hbar$ is Plank's constant divided by 2π, $\boldsymbol{M}$ is the mass matrix that holds on the diagonal the masses belonging to the atomic Cartesian degrees of freedom, and $\boldsymbol{\sigma}$ is the covariance matrix of atom positional fluctuations:

$$\sigma_{ij} = \left(x_i - \langle x_i \rangle \right) \left(y_i - \langle y_i \rangle \right) \quad (9)$$

Two separate trajectories (for example free and complex trajectories of a peptide) can be combined, thus one trajectory can be appended at the end of the other trajectory, and the plot of configurational entropy S against time can be used as assessment of the overlap between configurational spaces sampled in two simulations [60]. Such trajectories have been derived for the backbone (bb) atoms (N, C^{α}, C') of the peptide from the last 10 ns of the free (f) and bound (b) trajectories. Both appending sequences were applied resulting in S_{bb}^{f+b} and S_{bb}^{b+f} calculations, where the bound trajectory was appended to the free (f+b), or the free trajectory was appended to the bound one (b+f). Plotting the calculated values of S from both the combined trajectories over time demonstrates the relative size and overlap of sampled trajectories. Plotting of S over time after the combination of two trajectories results in three cases [60], briefly described as:

1. S increases after appending one trajectory to the other, with a jump observed at this point. Thus, the two trajectories do not overlap, or there is only a small overlap between them.
2. S evolves smoothly after the appending of the trajectories, without an observable perturbation of the line of S over time, thus the two trajectories show significant overlap.
3. S curve increases during the time of the first trajectory, but decreases a little bit after the appending of the second trajectory. Thus, the second trajectory samples a smaller configurational space than the first one, which also contains the configurational space visited by the second one.

Such an analysis of the combined trajectories is more advantageous than comparing directly the configurational entropies of two independent trajectories and it can provide information about the extent of sampling overlap (if any) between two the trajectories. The coverage of the free trajectory with respect to the complex trajectory is:

$$\Delta S_{bb}^{b+f} \equiv S_{bb}(complex, peptide) - S_{bb}(complex) \quad (10)$$

and the coverage of the bound (complex) trajectory with respect to the free trajectory is:

$$\Delta S_{bb}^{f+c} \equiv S_{bb}(peptide, complex) - S_{bb}(peptide) \quad (11)$$

EQUILIBRATION AND CONVERGENCE

Convergence is a very important issue in MD simulations [62-65]. Smith *et al.* [63] studied α and β peptides in methanol for 5 and 50 ns. They used cluster analysis in order to assess the convergence of the simulations. Their study suggests that a good convergence criterion is the number of different clusters over time. Namely, if this cumulative number reaches a plateau then we can assume convergence of the simulation. This can be best done if two separate trajectories are compared, for example, starting from different starting positions. Lyman and Zuckerman have studied the Met-enkephalin peptide [65] using the implicit solvation method GB/SA for 100 ns. The authors used clustering and classification techniques in order to study the convergence of MD trajectories. Their results indicated the lack of convergence for this small flexible peptide. Grossfield *et al.* [62] studied the protein rhodopsin by comparing the results of 26 independent MD trajectories of 100 ns length. Despite the extensive MD simulation time (according to modern standards), the authors argued that they could not be able to describe the protein's dynamic in a quantitative manner. Moreover, they mentioned that even small loops at the surface of the protein were not well sampled. Their results may be a significant caution when interpreting results from short MD trajectories. All the previous studies indicated that plotting RMSD (Root mean square deviation) time series after fitting the MD frames to the starting coordinates might not be a good indicator of convergence. Thus, if the serious impact of convergence upon the implementation of the MD results should be taken into account, a significant effort must be done in order to ensure that the MD trajectories are well equilibrated and converged.

T-CELL ANTIGENS AND RECEPTORS

The use of computational methods in immunology research has been termed immunoinformatics [66-68]. These techniques mainly aim at producing new vaccines. Vaccine discovery requires multidisciplinary combinatorial scientific approaches. Computational methods are a significant component, where substantial computer power is required [25, 66, 69], especially, if structure characterization is at the table. However, most of these prediction methods are sequence-based scoring function techniques [67], although some of them are coupled with other optimization techniques

[70]. Despite being very useful, these methods have certain limitations. Energy based approaches, such as molecular mechanics and interaction energy scoring can add valuable information to sequence based results [71-74]. So, MD simulations coupled to sequence-based information have been utilized in order to enhance the predictive power of the peptide affinity calculations to MHC molecules [69, 75]. Some interesting paradigms are highlighted below.

Studies Based on Class I MHC Molecules

Molecular dynamics simulations of a peptide bound to MHC molecule go back to 1992 [76]. Rognan *et al.* studied the complexation of the influenza-virus-matrix-protein (IMP) 58-66 nonapeptide, bound to the MHC HLA-A2. The nonapeptide GILGFVFTL was manually docked into the binding groove of the HLA-A2 molecule and molecular dynamics were performed with AMBER for 100 ps [76]. The simulation is very short for nowadays standards, but it was a breakthrough for that time. The authors observed several peptide/protein interactions and also some water mediated hydrogen bonds. Their results seem to be corroborated by x-ray studies of a relevant HLA-B27 complex [77].

MD simulations have been utilized in order to elucidate the difference between HLA-A*0217 and HLA-A*0201 in peptide binding. The two alleles differ in three residues at positions 95, 97 and 99 in the β-sheet floor of the MHC binding groove. It was found that Pro at position p3 occupying the F binding pocket was an optimum residue to lock the dominant anchor residue (phenylalanine at position p9) tightly into pocket F and to hold the peptide in the binding groove, rather than a secondary anchor residue fitting optimally the complementary pocket [78].

Another study of HLA-A*0201 binding peptides has been performed by Joseph *et al.* [79]. In this paper a series of GP2 peptide (IISAVVGIL) peptide were investigated in terms of binding affinity with the HLA-A*0201 molecule. The authors modeled various peptide/MHC complexes based on the GP2/HLA-A*0201 x-ray structure [80] and performed short (0.2 ns) MD simulations to explore the interactions between the peptides and MHC molecule. According to the resulted MD trajectories, low binding affinity of the GP2 peptide to the HLA-A*0201 molecule was ascribed to the conformational instability of the peptide within the MHC's binding groove. High RMSD values as of 4.5 Å were observed, and the peptide quickly lost its initial conformation. In consistence with x-ray data [80] the authors observed very high mobility of the central region of the peptide, residues p5-p7. This facts indicates the low affinity of the hydrophilic central floor of the HLA-A*0201 molecule for the Val_5 and Val_6 side chains of the peptide. The authors also observed a destruction of the Ile_9/MHC interactions, located at the "F" binding pocket, which are crucial for peptide binding. Replacement of Val_6 with hydrophilic residues (Ser, Thr or Asn) was tried out as a step to enhance the binding affinity. Relatively good results were obtained only from Val→Asp replacement, as tested by fluorescein isocyanate-labeled β2m binding experiments. MD simulations indicated that the side chain of Asn residue was oriented upward and the space created between the peptide and the MHC molecule could be filled with water that can act as hydrogen bond mediator [81]. Another point mutation that was found to enhance peptide binding was Gly→Phe at position p7. It is well known that Phe residues play important role in protein/protein interfaces [82]. MD simulations showed that this could be attributed to favorable interactions with MHC's Val_{152} side chain, which remained stable throughout the whole MD trajectory. Double mutations of the peptide's sequence did not reveal any improvement on the binding affinity, indicating the non-additive effect of the mutations. Although the short MD simulations of this study should be interpreted carefully, the authors were able to identify useful point mutations on the GP2 peptide and produce evidence of the enhanced binding affinity that corroborates with the experimental data [79].

HLA-B*2705 has been connected with the AS (Ankylosing spondylitis) disease [83]. This molecule differs by HLA-B*2709 in one single amino acid at position 116 (located on the floor of the MHC binding groove): HLA-B*2705 has Asp residue where HLA-B*2709 has His residue. It is very interesting that HLA-B*2705 is not associated with AS. Both these MHC molecules have been crystallized in the presence of the RRKWRRWHL peptide [84], derived from the sequence 400-408 of the vasoactive intestinal peptide type 1 receptor. The x-ray structures of these complexes provide one of the most striking examples of peptide's conformational flexibility in immunology. It was found that in the pVIPR/HLA-B*2705 complex the peptide adopted the canonical conformation, while in the pVIPR/HLA-B*2709 complex the peptide had adopted two conformations "A" and "B". Conformation "A" was also in the canonical binding form, while in the conformation "B" the peptide was allowed to form a salt bridge between peptide's Arg_5 and Asp_{166} from MHC's heavy chain. Despite the difference in peptide's conformation, the MHC molecules were found in virtual the same conformation [84]. However, CTL (Cytoxic T lymphocytes) with specificity for HLA-B27 molecules presenting the pVIPR peptide are very frequently found in normal individual bearing HLA-B*2705, and even more in patients with AS, while they are only rarely found in HLA-B*2709 carriers [83]. Fabian *et al.* carried out isotope edited (^{13}C) IR spectroscopic studies in order to measure flexibility of the heavy chain of the MHC molecule in both HLA subtypes. Their results revealed an increased mobility of the α-helical segment of the HLA-B*2705 relatively to HLA*B2709. Since the available x-ray structures of the pVIPR/MHC complexes cannot explain these differences, the authors carried out extensive (40 ns) MD simulations of the complexes [85] using the GROMACS software. HLA-B*2705 complex was simulated with both conformations found in the x-ray: the canonical and the non canonical one. The authors analyzed the MD results from RMSF perspective and measured the flexibility of MHC's heavy chain, as compared to experimental derived B-factors (Fig. **1**). A very interesting outcome of their investigation was that the complexes with the pVIPR peptide in canonical conformations revealed different flexibilities. The HLA-B*2705 showed considerably increased backbone flexibility of the heavy chain, in comparison with HLA-B*2709, despite the fact that the pVIPR/HLA-B*2705 has been observed to have grater thermostability relatively to the pVIPR/HLA-B*2709 complex. In contrast, the flexibility of HLA-B*2705 with peptide in non-canonical conformation was found similar to those of HLA-B*2709. So, it can be

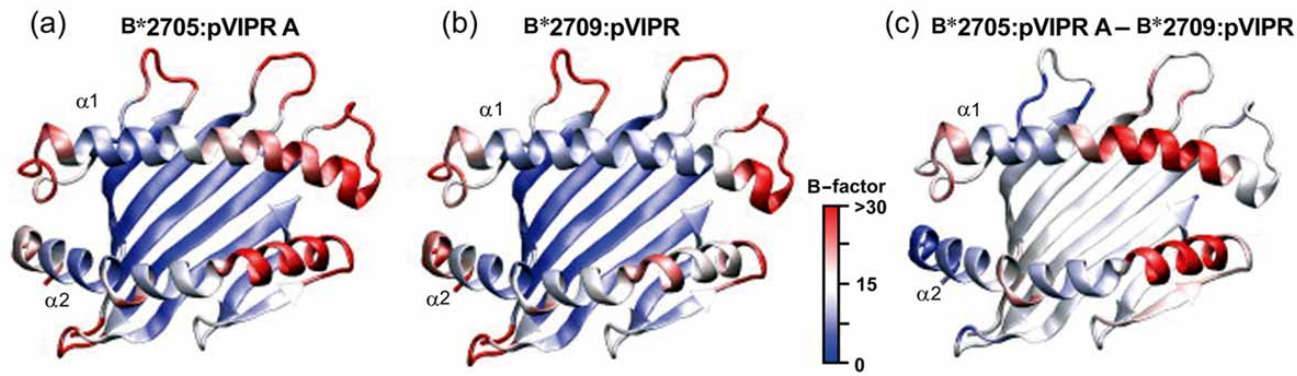

Fig. (1). Dependence of conformational flexibility of the MHC binding groove on HLA subtype. Fabian *et al*. performed MD simulations on HLA-B*2705 and HLA-B*2709, two HLA subtypes that differ only in one residue: Asp *vs* His respectively at position 116 of the α chain. Both molecules were complexed with the RRKWRRWHL peptide (pVIPR). MD runs were performed for 40 ns in explicit water with GROMACS. Theoretical values of B-factors were extracted from MD trajectories with according to the formula $B=8/3\pi^2$ $rmsf^2$. Subfigures **a**) and **b**) displays the calculated flexibility of the B*2705 and B*2709 binding grooves respectively, while subfigure c) shows the flexibility difference. Reproduced after permission from Elsevier Ltd. J Mol Biol (2008), 376:798-810.

concluded that the differences revealed by IR spectroscopy is due to peptides bound with the canonical conformation. While the relevance of the results from this work with the association of AS with HLA-B*2705 and HLA-B*2709 remains controversial, the combination of experimental and theoretical techniques by Fabian *et al.* [85] demonstrated the value of these multidisciplinary approaches.

Class I H-2K^b

Lazoura *et al.* [86] presented a modeling study of Strp9 peptide bound to MHC molecule. The SRDNSRIPM sequence (Strp9) was modeled based on the x-ray structure of the YEA9 (SRDHSRTPM) peptide bound to the same MHC molecule. By applying a short MD simulation the authors were able to identify the binding mode of the Strp9 peptide. However, this study revealed that the Strp9 peptide binds less tight to the MHC H-2K^b molecule due to lower hydrogen bond potential, relatively to YEA9 peptide. They have also noted that this happens despite the presence of large anchoring residues, Arg-p2 and Met-p9, in addition to Arg-p6 in the E pocket, which plays a major role in enabling high affinity binding of the peptide to H-2K^b. Thus, the non-canonical Strp9 peptide appears to bind with the same anchoring amino acids utilizing the new-E pocket. However, the decreased potential for hydrogen bonding of Strp9 in the H-2K^b binding groove is likely to account for the lower binding affinity and induction of lower avidity T cells when compared to the YEA9 peptide.

Studies Based on Class II MHC Molecules

The YWALEAAAD peptide has been studied in complex with HLA-DR4 (HLA-DRB1*0405 allotype) with both MD simulations and T cell proliferation assays [87]. Toh *et al.* carried out extensive amino acid substitutions in this sequence at positions p3, p5, p7 and p8 (anchor residues). The peptides were classified as agonists, antagonists and null (non-agonists and non-antagonists) depending on the response pattern of T cell clones. The study revealed that a Glu residue was absolutely necessary at position p5 for TCR recognition, and that even a conservative mutation of Glu→Asp at position p5 could be recognized differently by the TCR. The peptide with Glu residue at position p5 was classified as a strong agonist, while the peptide with Asp at position Asp was identified as a weak antagonist. The authors also identified major conformational shifts in the β-chain helix after residue replacements at position p7, which maybe be related with experimental data that show more potent effects on p7 replacements.

Knapp *et al.* presented a combined study of peptide/MHC interactions utilizing *in silico* prediction methods, competition assays and T cell cultures [74]. Two peptides derived from Art v 1 protein, the major mugwort pollen allergen, with sequences KCIEWEKAQHGA (12mer, Art v $1_{25\text{-}36}$) and NKKCDKKCIEWEKAQHGA (16mer, Art v $1_{19\text{-}36}$) respectively, were modeled in the binding groove of the HLA*DRB1*0101 allele. The authors used the NetMHCII software to identify Ile_{27} as the p1 anchor residue for both peptides. Then, the peptides were adjusted in the binding groove of the MHC molecule and the author performed MD simulations (20 ns with GROMACS) combined with energy minimization to obtain reliable peptide/MHC structures. Analysis of the results based on RMSD time series revealed that the complexes were quite stable. The total number of hydrogen bonds between the peptides and the MHC molecule was also calculated through out the MD trajectories. The obtained median values were 10 and 16 for the 12mer and 16mer peptides respectively. The corresponding normalized values were 0.83 and 0.87, if the peptide sequence is taken into consideration. Furthermore, calculation of binding affinity score with Xscore revealed the values of 7.7 and 9.6 for 12mer and 16mer peptides respectively, when the calculations were performed for the last 5 ns of MD simulations. From these results it was concluded that the 16mer peptide (Art v $1_{19\text{-}36}$) has a stronger affinity to HLA-DRB1*0101. Biological experiments with T cell lines and T cell clones confirmed this fact. Interestingly, the MD simulations revealed another important feature of peptide's conformation: the six residue extension (NKKCDK) of the 16mer peptide from the N-terminal part of the peptide sequence was folded into a loop-like structure, which allowed for extra peptide/MHC interactions, outside

of the core peptide/MHC binding grove. Zavala-Ruiz *et al.* [88] have also reported an x-ray structure of a hairpin-turn 16mer peptide bound at MHC class II molecule, that has stronger binding affinity in comparison with a 13mer peptide, although the extension was from the C-terminal part. The study of Knapp *et al.* [94] corroborate the idea that extended peptide sequences may have better binding affinities for MHC class II molecules. Moreover, the authors demonstrated the use of MD simulations as a useful insight tool to peptide/MHC interactions that reveal a lot of structural information of peptide/MHC association in contrast to sequence based tools.

Mantzourani *et al.* [89] presented an MD study of the MBP (Myelin basic protein) epitope 87-99 in complex with HLA-DR2b. Along with the native sequence (E_{83}NPVHFFKNIVTPR$_{97}$) the authors also studied two antagonist peptides: [Arg_{91},Ala_{96}]MBP_{87-99} and [Ala_{91},Ala_{96}]MBP_{87-99}. Despite the relatively short (2 ns) MD simulations in explicit water performed with AMBER software, the authors were able to determine significant conformational changes among the three peptides bound to HLA-DR2b. The complexes with the ten lower energies were isolated from MD trajectories and calculation of SASA was utilized in order to determine whether residues are buried or exposed in each conformation. For the native x-ray structure complex, no major conformational changes were observed over the 2ns simulation. However, for the two APLs (Altered peptide ligands) it was found that once bound to the MHC, significant changes occurred in the orientation of the amino acids that serve as TCR anchors. In both APLs the TCR anchor Phe_{89} is buried in all conformers. TCR anchor residue His_{88} is buried in most of the conformations for the [$Ala_{91,96}$]MBP_{87-99} complex. This residue was found moderately buried in the [Arg_{91},Ala_{96}]MBP_{87-99} complex, however it was found in a notably different orientation with respect to the x-ray structure (Fig. **2**). Both human autoimmune TCRs primarily recognize the N-terminal, unlike all other TCRs that bind over the central portion of the peptide. From MD analysis the authors also concluded that the peptide action as antagonists comes from the lack of the N-terminal part of the native peptide that possibly acts as first contact for the TCR.

Software Tools to Employ Massive MD Simulations and/or Analysis of Results

Nowadays, there is a considerable effort to assist the prediction of peptide binding to MHC molecules with MD simulations and to overcome the deficiencies of sequence or motif predicted methods. Recently, Todman *et al.* [69] presented a software tool (MHCsim, http://igrid-ext.cryst.bbk.ac.uk/MHCsim) that allows the automated construction of MHC/peptide structure files and the corresponding configuration files required to execute an MD simulation using NAMD [39]. The system has been made available through a web-based front end and stand-alone scripts. This can be used to virtually any peptide/MHC complex and not only to specific alleles. The authors presented thus a framework where one cannot only perform MD simulations, but to use these techniques to extract binding affinities. This can be accomplished by ABF (Adaptive biasing forse), FEP (Free energy pertubation) or TI (Thermodynamic Integration) MD simulations. Utilization of these methods has considerable cost in terms of computational time and power in comparison with sequence based methods, however it provides better validity of structure based affinity calculations for peptide/MHC binding [72]. The authors used the software on four different datasets, each containing 15 combinations of structures. In the first dataset, they compared structures of HLA-A*0201 generated by MHCsim using the A*1101 templates against genuine A*0201 structures. In the second, they compared random combinations of A*0201 structures. In the third dataset, they compared random combinations of MHC Class I structures and in the fourth dataset they compared random combinations of MHC Class II structures. Then, by performing MD simulations, the authors were able to reproduce peptide/MHC structures comparable with the known x-ray structures with reasonable precision. It is notable that web-based access (http://igrid-ext.cryst.bbk.ac.uk/MHCsim) to this software tool might be very useful to experimentalists [15] with limited training in MD simulations, especially at the crucial first step: preparation and set up of the peptide/MHC complexes for MD simulations. This step involves many human-controlled parameters [21] and the wise use of them can affect drastically the quality of the simulation.

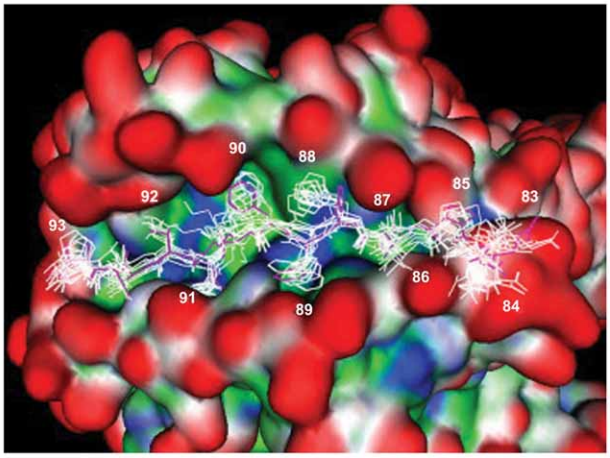

Fig. (2). The MBP83-96 peptide bound to HLA-DR2b molecule. Superimposition of the ten lowest energy peptide conformations as obtained from MD trajectory on the native peptide (colored purple). Red color corresponds to exposed regions of the MHC molecule, while blue and green correspond to hydrophilic and hydrophobic regions respectively. Reproduced after permission from Elsevier Ltd. J Mol Graph Mod (2007), 26:471-481 (For interpretation of the references to color in this figure legend, the reader is referred to the web version of this paper).

Another structure-based prediction method of peptide binding to MHC class I molecules has been published by Fagerbrg *et al.* [75] based on MD simulations and simulated annealing. The authors used an extensive data set of peptide/MHC complexes obtained from Protein Data Bank. Their method consisted of multiple steps. In the first step, after building the initial model, they utilized simulated annealing (1300 K) to accelerate the conformational space sampling combined with adopted basis Newton-Raphson energy minimization. By repeating the dynamics/mini-mization cycle they obtained 1000 representative conformers

of the peptide/MHC complex. Then, they performed cluster analysis to the resulted conformers based on RMSD calculations. In a third step the authors calculated the effective energy of the conformers (see methods of ref. [75] for details).

Predicting the MHC binding affinity of a peptide is not a trivial task, neither experimentally nor computationally. Todman *et al.* [69] suggested a general method for calculating ΔG of binding based on MD simulations [47]. The authors presented a software tool written in Perl that enables the construction of any peptide/MHC complex of any HLA allotype and the creation of PDB and PSF (Protein structure file) files. The user can define the HLA allotype and the peptide sequence that is of interest. The software tries to model the structure based on the available x-ray structures. After finding the closest match by pairwise alignment the software performs any required mutation to match the user defined input sequence of both the peptide and allotype. The complexes are suitably solvated and after defining few parameters the software can produce the NAMD configuration files that are used for MD or ABF simulations. Users that have access to big computer clusters or grid services can find this application particularly useful, since it allows the automation of structure preparation and MD configuration of multiple peptide/MHC complexes that can be studied in order to calculate the ΔG of binding. This method can potentially substitute the heavy laboratory work needed to define a T-cell epitope of protein with the method of the overlapping peptides.

Water Structure in Peptide/MHC Complexes

Beyond the prediction of peptide binding to MHC molecules, MD simulations have also been used in order to elucidate the role of water in peptide/MHC association. The peptide ILKEPVHGV derived from the reverse-transcriptase sequence of HIV was used in a model study, in complex with the MHC-HLA-A2 [73]. In this study, Petrone and Garcia performed MD simulations of the peptide/MHC complex as well as the MHC molecule without the peptide in order to determine the role of the solvent in peptide binding, something that has been noticed in other cases as well [90, 91]. To quantify their results they introduced the calculation of the instantaneous water calculation number, by calculating the number of water molecules within a 3.5 Å cutoff from water oxygen atom, at every saved snapshot from the MD trajectory. Basically, this is first hydration shell and typically it has a value of approximately 4-6 for bulk water. In the proximity of protein atoms this number drops, and we can consider a water molecule as protein-bound, if this number is less than 3. Analysis of the MD trajectories revealed very interesting facts about the role of water at the peptide/MHC interface. Some other water molecules were found to retain stable positions within the peptide/MHC complex for at least 1 ns or longer. These water molecules made specific interactions between the peptide and the *β*-sheet floor of the MHC molecules. Some other were molecules were bound at the charged N- and C- terminals of the peptide, thus facilitating the binding without being specific to any particular peptide residue. Free energy calculations also revealed that water molecules affect the binding ΔG. In comparison with the simulation of MHC molecule in the absence of the peptide, the authors concluded that the water molecules assisted the MHC molecule to exhibit plasticity in the absence of the peptide and to adapt the conformation of side chain atoms to maximize peptide contacts.

Peptide Free Models of MHC Molecules

There is a growing interest to construct peptide-free MHC models. Recently, Painter *et al.* [92] presented a molecular modeling study coupled with extensive MD simulations of the HLA-DR1 MHC molecule. They used the x-ray structure of the class II MHC molecule complexed with the PKYVKQNTLKLAT peptide (PDB code: 1sje) to generate a model of peptide free MHC molecule by manually removing the peptide from the PDB file. The protein was solvated in a water box, and after minimization/equilibration, the system was subjected to a 60 ns MD simulation with GROMACS. The authors also took care of the convergence of the simulation [93]. Their study revealed an interested future of the MHC molecule: without the loaded peptide the α50-59 region of the MHC molecule gradually lost its helical conformation and moved towards helix β of the MHC molecule. Thus this part of protein occupied the position of the peptide region p1-p4, adopting also the peptide's conformation. This theoretically produced result was corroborated by binding affinity experiments with the conformationally restricted LB3.1 monoclonal antibody [92].

A similar study by Yaneva *et al.* [94] was published almost simultaneously with the previous one. The authors performed MD simulations of the HLA-DR3 molecule in the absence and presence of the peptide PVSKMRMATPLIMQA (PDB code: 1a6a). Simulation of this MHC class II molecule in peptide free form also revealed significant conformational mobility of the helical region in the peptide binding groove. However, in contrast with the α50-59 region in the HLA-DRB1 case, the most flexible part of the HLA-DR3 molecule was located in the β58-69 region, in the proximity of the p4-p6 peptide binding sites.

PEPTIDE – ANTIBODY COMPLEXES

Antibodies are capable to recognize a big variety of molecules [95]. Antigen binding topography [96] has been attributed to six fragments that constitute the Complementary Determining Regions (CDRs). Complexation of antibodies with antigens has been also associated with the so called hot spots [82, 95, 97]. There are several examples of applications of MD to immunogenic peptides [98, 99], although, simplified models for studying peptide/antibody complexation have been employed as well [100]. Some of the most interesting examples are given below.

Peptide Epitope Mimicry

Myasthenia gravis is caused by autoantibodies against the AChR (Nicotinic acetylcholine receptor) of the neuromuscular junction and a small region on the extracellular part of the AChR alpha subunit seems to be the major target of the anti-AChR antibodies. The major loop of the overlapping epitopes for all testable anti-MIR (Major

immunogenic region) monoclonal antibodies was localized within residues 67-76 (WNPADYGGIK for Torpedo and WNPDDYGGVK for human AChR) of the alpha subunit [101, 102]. The N-terminal part of the alpha 67-76 peptide is the most critical one, where residues Asn_{68} and Asp_{71} are indispensable for binding. Orlewski *et al.* [103] presented acombined NMR (Nuclear magnetic resonance) and MD study of an analogue peptide [Ala_{78}]MIR, in free and antibody bound states. In consistency with previous reports [101], the authors reported the conformationally controlled binding of the [Ala_{78}]MIR by monoclonal antibodies. It was found that the N-terminal part of peptide formed a type I β-turn in the free state and a type III β-turn in the bound state. This conformational change has been stated as crucial in the binding process. In continuation of this work, Kleinjung *et al.* [103] have studied the complex between an Fv antibody fragment and a peptide analogue [Gly_{70},Nle_{76}]MIR of the acetylcholine receptor with 2D-NMR, homology and molecular modeling. The authors performed also restrained MD simulation for 750 ps of the peptide/antibody complex based on their NMR derived NOE interactions. This served as a relaxation process after homology building of the antibody structure and docking of the peptide into antibody's binding site. Certain parts of the peptide's sequence were found quite mobile within the antibody's binding site, although, the biggest flexibility showed the H3 loop of antibody's CDRs [103]. The [Gly_{70},Nle_{76}]MIR peptide was found to retain its β-turn structure at the N-terminal part as in the [Ala_{78}]MIR case ant in agreement with other peptide/antibody structures [104]. However, the authors observed a destruction of the type III β-turn due to a different backbone conformation adopted by the Gly_{70} residue. The flexibility of this residue should have contributed to binding enhancement (Fig. **3**). It has to be noted that the antibody was raised against the human AChR, but also binds the [Gly_{70},Nle_{76}]MIR peptide with high affinity. Thus, the peptide's conformation probably mimics well the conformation of the protein at the 67-76 region, an essential prerequisite for peptide immunogenicity [105]. In these studies MD simulations helped to identify structural elements of the peptide's conformation and to build up a model of the antibody/antigen complex.

Thermodynamics of Peptide's Immunogenicity

MD simulations have been also used in order to study the thermodynamics of peptide's immunogenicity. It is expected that antibodies raised against peptides should recognize also the corresponding region of the native proteins [106]. This can be done by assuming that a peptide can adopt a stable conformation in solution, similar to that of the corresponding region in the native protein. It has to be noted that it is not the binding to an antibody that is important for the design of immunogenic peptides, but rather the molecular mimicry of the unbound peptide to the cognate antigen [105]. Sometimes this can be accomplished by peptide cyclization as shown by Oomen *et al.* [98]. Camacho *et al.* [107] presented an MD study coupled with immunization experiments involving peptides (Fig. **4**) from the HRS (Histidyl-tRNA antigen) autoantigen. Their study aimed establishing a thermodynamic basis for linking peptide immunogenicity with native protein motifs. According to their analysis, peptide conformations can be classified in three categories according to the free energy (ΔG_x) of their protein-like motifs: a) $\Delta G_X<0$ kcal/mol that can form the same number of peptide-antibody complexes, b) $\Delta G_X>0$ kcal/mol, $\Delta G_X<8$ kcal/mol that have a significantly reduced capability of inducing antibodies relatively to native proteins and c) $\Delta G_X>8$ kcal/mol for unstable "non-immunogenic" peptides. Within this context, Camacho *et al.* [107] employed 10 ns MD simulations studies of ten 18mer peptides derived from the N-terminal part of the HRS autoantigen in searching for structural stability of the corresponding peptides. The authors analyzed the MD results from RMSD perspective (in relation with the starting conformation) and the number of hydrogen bonds that stabilized the peptide's structure. Then they classified the peptide's stability and related the results with ELISA experiments. It was found that peptides with relatively stable conformations, that shared the same conformational characteristics of the native protein, were capable of inducing anti-protein antibodies. The authors were also able to fully correlate the biological activity of the peptides with their structural stability, demonstrating the power of MD simulations as predictive tool of immunogenicity. For example, peptides 9 (sequence 81-98 of HRS) and 10 (sequence 91-108 of HRS) showed considerable difference in antibody binding, with peptide 9 having much greater affinity than peptide 10 (Fig. **4**). This happens despite the fact that both peptides share the highly immunodominant proline containing epitope of the 93-96 region. The ELISA results were fully compatible with the MD studies: the peptide 9 retained its conformational stability while peptide 10 was considerably destabilized during MD trajectory.

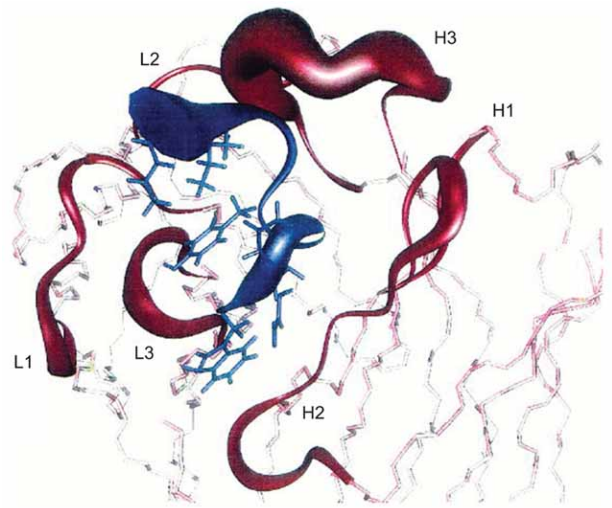

Fig. (3). The peptide WNPADYGGIK corresponding to the 67-76 region of the AChR sequence has been modeled in the presence of a monoclonal antibody. NMR studies and MD dynamics simulations were utilized in order to explore the dynamics and the flexibility of the binding mode. The scale of the backbone ribbon rendering is proportional to the mobility of the backbone. Reproduced after permission from John Willey & Sons Inc, Biopolymers (2000) 53:113-118.

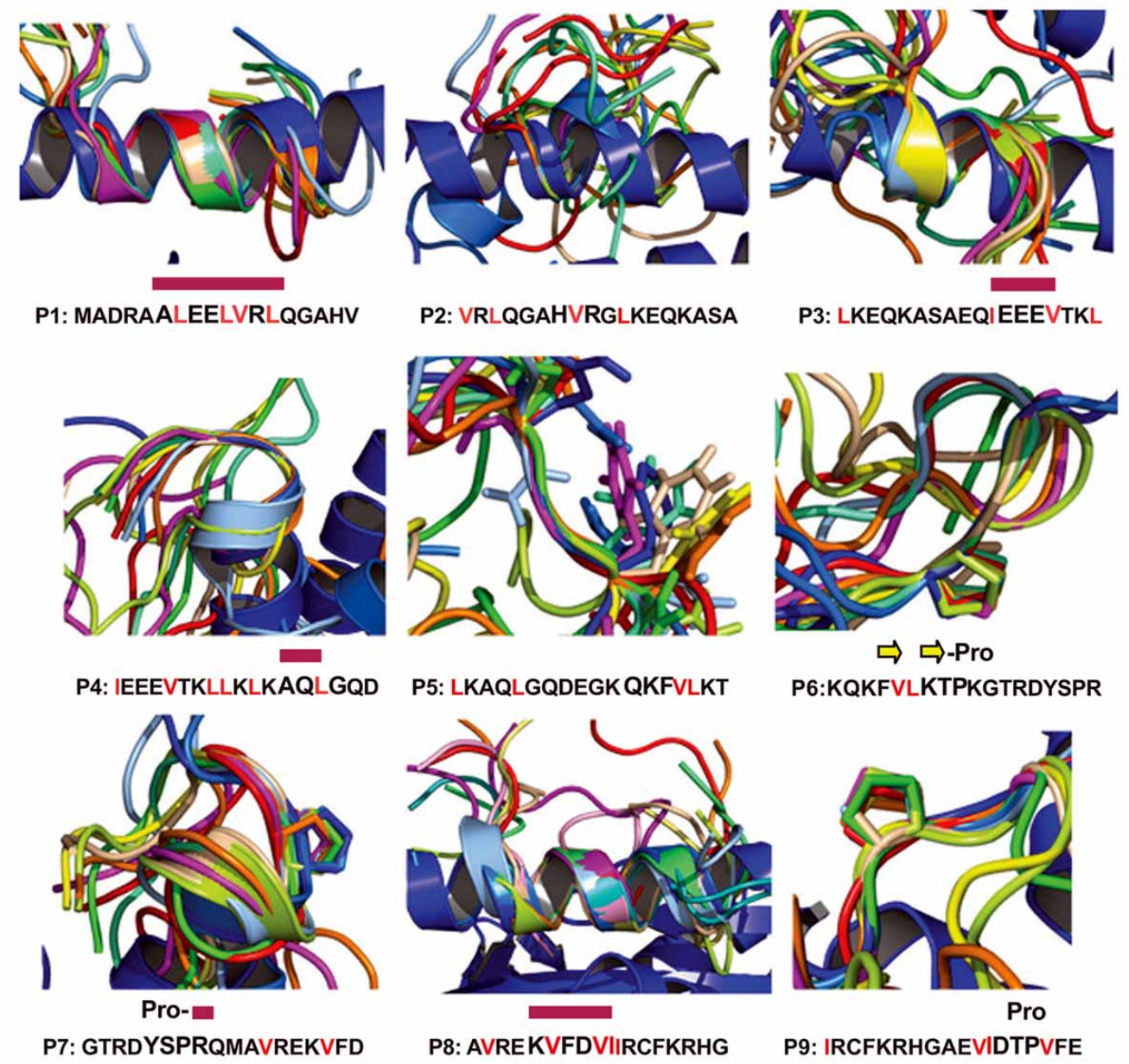

Fig. (4). Camacho *et al.* extracted 10 18mer peptides from murine HRS sequence as B-cell epitopes and performed MD simulations in order to evaluate their structural stability. The figure shows snapshots (every 1 ns) from 10 ns MD simulations of the superimposed peptide structures. Reproduced from PloS Comput Biol (2008), 4: e100231.

Cyclization of Peptides

Oomen *et al.* [98] presented a study that best illustrates the use of MD simulations for predicting conformationally restricted epitopes. In stead of trying to improve binding of peptide to antibody, the authors employed MD simulations to stabilize to secondary structure of a peptide and to enhance its solution conformation to those of the native protein. PorA porin protein from Neisseria meningitis has been predicted to contain eight surface-exposed loops [108] and monoclonal antibodies have been found to react with peptide epitopes located at these loops. Moreover the peptide TKDTNNNL derived from the 180-187 sequence of PorA protein has been crystallized in presence of a Fab fragment from a bactericidal antibody specific for PorA P1.16 subtype [109] (see http://neisseria.org for naming convections). The peptide adopted a β-hairpin conformation in the bound state. Several peptides were designed in order to stabilize this secondary structure *via* head-to-tail cyclization. The designed sequences incorporated the Tyr-Asn-Gly-Lys fragment as the contra-turn region to facilitate cyclization [110, 111]. Turns are well known structural motif that stabilize β-hairpin conformation in designed peptides [110]. In some cases Tyr were replaced with Cys to facilitate conjugation of the peptide with a carrier protein. The

structural stability of the designed β-hairpin peptide was evaluated by 10 ns MD simulations in explicit water. The conformational mimicry of the bound antigen by the cyclic peptides was assessed by monitoring the presence of characteristic hydrogen bonds. For example the existence Asp_3:H^N-Asn_7:O hydrogen bond that characterized a 3:5 type I β-turn in the bound to antibody peptide has served as a measurement of how similar the peptide conformation was to the epitope's structure (Fig. **5**). It was found that two out of four studied peptides could not retain the desired conformation and they showed no structural stability. The third peptide however, retained the desired β-harpin conformation and the Asp_3:H^N-Asn_7:O hydrogen bond for the 58% of the simulation time. The fourth peptide showed considerable backbone flexibility though also partly retained the β-harpin conformation for 38% of the time. The peptide preference for an ordered β-harpin structure offered the authors a mean to classify the four designed peptides in terms of molecular mimicry of the native antigen. Binding assay experiments were performed in order to evaluate the peptide preference for antibody binding. It was found that biological activity followed precisely the pattern assumed from MD simulations. Thus, the peptide showed the maximum β-harpin stability had the highest binding activity. Moreover this peptide was used in immunization experiments and was proved to elicit antibodies that activate the complement system resulting in bacteria killing. The work by Oomen *et al.* [98] provides a solid framework of rational structure-based design that seems to be superior to other trial-and-error methods [112]. In this approach, accounting the peptide flexibility seemed to play a crucial role, in which MD simulations correctly identified the best peptide candidate. It is also an example of β-turn therapeutics [113].

The same research group repeated the molecular mimicry approach to another case, two years later. Oomen *et al.* [114] presented the x-ray structure of the epitope peptide Ac-

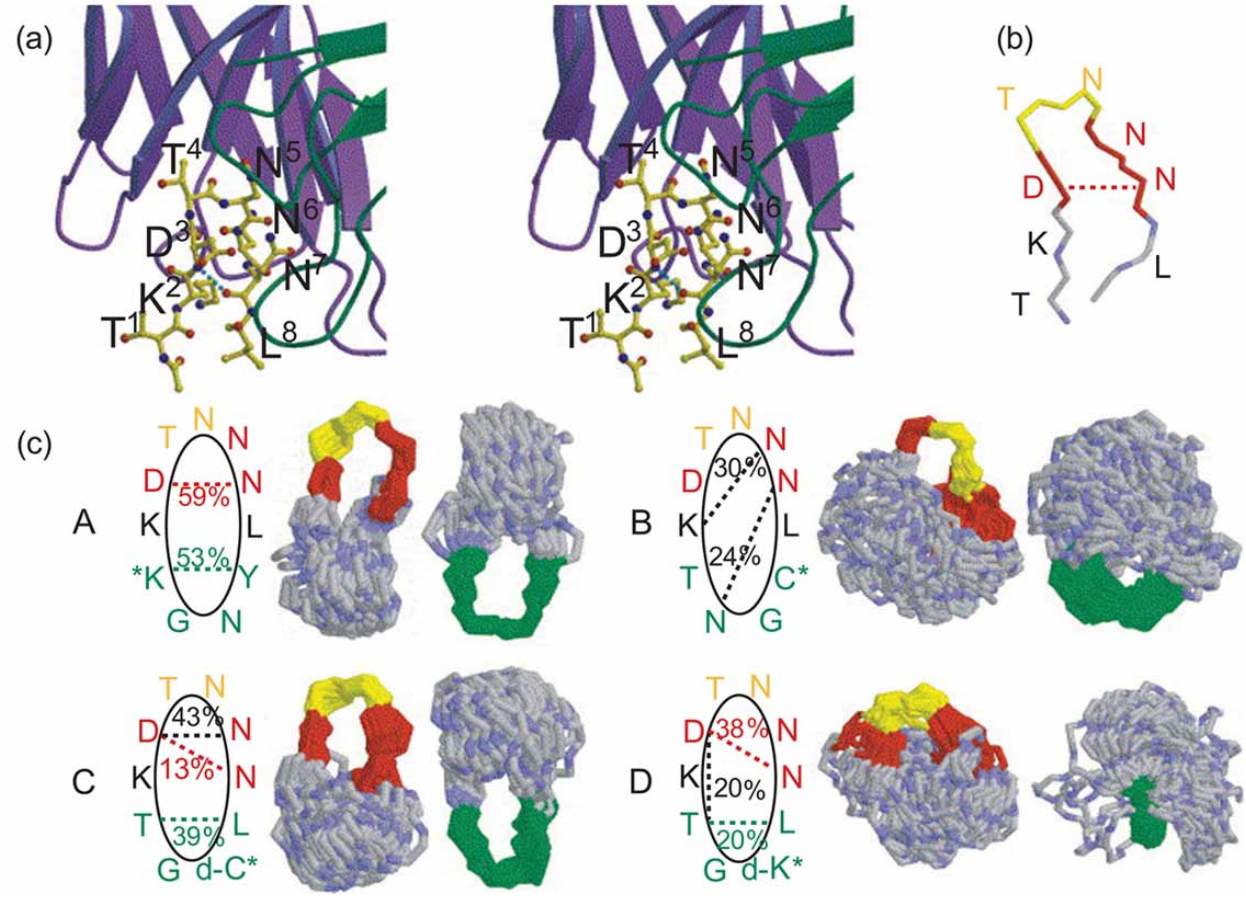

Fig. (5). Computational structure-based approach for design and evaluation of conformationally restricted peptide based vaccines presented by Oomen *et al.* The X-ray structure of the antibody/peptide complex in stereoview (**a**) and backbone conformation of the TKDTNNNL peptide (**b**) with a type I -turn at residues 3DTNNN7 (corresponding to residues 182-186 in PorA). Four peptide-vaccine **A**, **B**, **C** and **D** candidates were designed to mimic this conformation of the -turn peptide, shown in (**c**). Peptide sequences are shown with one-letter code for amino acids. To reduce the flexibility, the peptides were conformationally restricted by head-to-tail cyclization, adding some extra residues to construct the contra-turn with high propensity to form a -turn. Molecular dynamics simulations of the peptides were employed to assess the conformational mimicry of the peptides to the crystallographically observed -turn. Snapshots of the peptides during the molecular dynamics simulation run were superimposed on either epitope-turn (red and yellow) or contra-turn (green). The conformational mimicry is assessed by the presence in the simulation of the desired backbone (red and green dotted lines) and undesired (black dotted lines) hydrogen bonds; the percentages of simulation time for observed hydrogen bond formation are included in the representation of the designs. Reproduced after permission from Elsevier Ltd., J Mol Biol (2003), 351: 1070-1080 (For interpretation of the references to color in this figure legend, the reader is referred to the web version of this paper).

HVVVNNKVATH-NH_2 bound with the anti-P1.4 antibody MN20B9.34. The bound peptide was found in *β*-hairpin conformation stabilized with three intramolecular hydrogen bonds. Based on the previously analyzed successful approach, the authors designed two cyclic peptides, with sequences NGKVNNKVAY and dCGVVNNKVAT respectively, in order to mimic the peptide's *β*-hairpin conformation in solution. This was performed with the aim to elucidate antibodies capable of cross-reaction with the original pathogen. The authors performed MD simulations for 5 ns of both in order to test their conformational stability and their preference for *β*-hairpin conformation. It was found that both peptides retained the desired *β*-harpin conformation and the initial *β*-turn structure around the NNKV fragment for substantial amount of the simulation time. Both cyclic peptides were synthesized and tested with immunization experiments (immunization of 8 mice). The results obtained from these immunological studies were widely divergent. For the first peptide, sera from three mice were found with high bactericidal titres, while for the second peptide, four mice responded to immunization but with lower titres. Interestingly, the subset of mice that responded to peptide 1 immunization produced antibodies capable of killing the bacteria. The lack of universal response to peptide immunization is not well understood and can be attributed to poor molecular mimicry of the peptides to the conformation of the pathogen. This is something that leaves place for further improvement of the peptide's immunogenicity through conformational stability. MD simulations might have a lot to offer towards this target, perhaps by prolonging the simulation time or by testing more compounds.

Cyclization may not be a Panacea

Another interesting example of peptide/antibody interactions comes from a peptide bound to CAMPATH-1H antibody, a humanized [115] monoclonal antibody against the CD52 antigen [116]. CAMPATH-1H has been used successfully for the treatment of leukemia, autoimmune disease and transplant rejection [117, 118]. The CAMPATH-1H antibody has a highly basic binding site. It has been shown that the antibody binds the peptide mimotope $T_1SSPSAD_7$, and the complex structure has been determined by x-ray [119]. The peptide's conformation in bound state was found to be type I *β*-turn around Pro_5-Ser_6 residues. In contrast to other cases, where the CDR-H3 is essential to antigen binding [96], the CDR-L3 of CAMPATH-1H dominates antigen binding [119]. MD simulations have been performed for the peptide/antibody complex as well for the free peptide in explicit water to determine the stability of the *β*-turn conformation [120]. The MD simulations confirmed the importance of electrostatic interactions between peptide's Asp_7 residue at C-terminal and antibody's Arg_{H52} residue. Moreover, the turn structure in the central part of the peptide was very well conserved during the 10 ns of the simulation. On the contrary, when the peptide was simulated in the free state it abolished the turn structure quickly. The initial conformation was retained for less than 5% of the 50 ns trajectory. This study demonstrated the well known induced fit procedure for antibody binding process [95], although the conformational change applies here to the antigen and not to the antibody. The turn structure of the $T_1SSPSAD_7$ peptide when bound to the CAMPATH-1H antibody and the close proximity of Thr_1 and Ala_6 side chains in peptide's conformation, led to the assumption that a possible cyclization through these side chains could stabilize the *β*-turn structure, and thus, enhance the binding properties of the $T_1SSPSAD_7$ peptide. The peptide's residues Thr_1 and Ala_6 have been replaced with Cys and a disulfide bond was imposed. MD simulations in free and bound state have been performed in order to assess the feasibility of the model as well as the stability of the *β*-turn around Pro_4-Ser_5 fragment [121]. MD simulations showed the stability of the *β*-turn for considerable amount of simulation time (>90%) in both free and bound states. The similarity of the peptide's backbone conformation in these two trajectories has been measured in terms of backbone entropy with a method presented by Hsu *et al.* [60]. The entropy difference was estimated 0.15 kJ/K/mol, a relative moderate value, indicating that the two sets of conformations (free and bound states) do not differ dramatically [121]. However, the conformational similarity of the cyclic peptide between the free and the bound states did not resulted in better binding affinity. MD simulation of the bound compound showed considerable decrease of hydrogen bonds between the peptide and the antibody during simulation time. Moreover, calculation of BSA (Buried surface area) between peptide and antibody showed a decrease of approximately 25% during the MD simulation. Conformational transition that led to this BSA reduction occurred after the first 2.5 ns of the simulation (total time 20 ns) underlying the importance of long time sampling during MD. Taking all these into consideration, cyclization led to more stable peptide structure in the free state, but resulted in lowering of its binding affinity [121]. This is an example of how carefully structure stabilization of flexible peptides should be interpreted, and how cyclization of peptides should not be overemphasized for enhancing the binding and immunogenic properties of linear peptides.

OTHER IMMUNOLOGICAL COMPLEXES

Beyond epitope prediction and vaccine design, MD simulations have been used in other immunological complexes, such as the complement system [122, 123]. Human C8 is composed by three genetically distinct subunits: α, β and γ. C8α and C8γ form a C8 α-γ heterodimer which is linked through a disulfide bond and this in turn associates non-covalently with C8β [124]. Mapping the binding sites of C8α complement protein to other C8 subunits [125] has revealed a 19mer peptide to be responsible for C8γ binding. A smaller fragment of 11 residues (indel peptide) was also capable of biological activity. Recently, the crystal structure between C8γ and the indel peptide of C8α sequence has been published [126]. In this complex, both Cys40 of C8γ and Cys164 of C8α chains respectively were substituted by Ala residues. These two cysteine residues form the disulfide bond of the heterodimer C8α-γ. The peptide $L_{158}RYDSTAERLY_{168}$ is a minimal sequence from the C8α protein that binds to the C8γ. Interestingly, it contains the Cys_{164} residue that forms a disulphide bond with Cys_{40} of C8γ, when C8α and C8γ complement protein associate into a heterodimer. In order to check this hypothesis and further provide evidence the C8γ association with C8α derived peptide through disulfide bond, molecular modeling and MD simulation techniques were applied [127]. Starting from the C8γ/C8α indel peptide X-

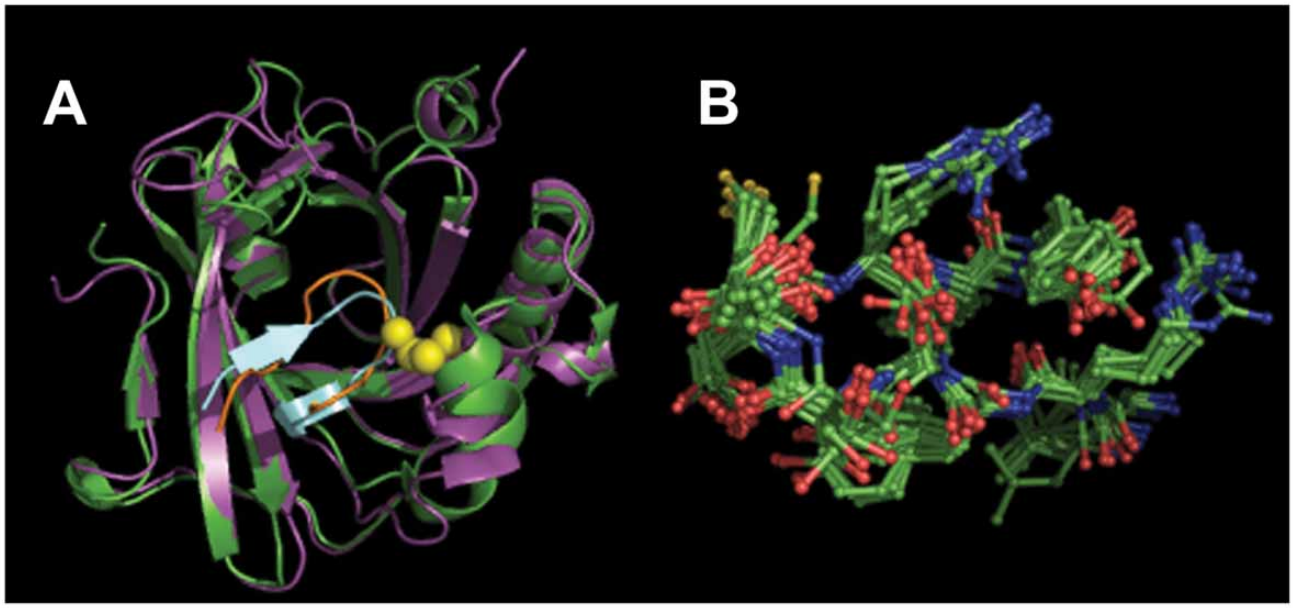

Fig. (6). A C8 indel peptide (LRYDSTAERLY) has been modeled in complex with the C8 protein. The x-ray structure was used as initial model to mutate two Ala residues into Cys and impose a disulfide bond that it is supposed to facilitate protein/protein heterodimerization in C8 /C8 complex formation. MD simulations were performed for 15 ns in order to assess the stability of heterodimer. **A**) Backbone atoms superimposition of the initial (x-Ray) and final (frame 15000) structures. The disulfide link (atoms C , S) is represented with balls. Chain C (C8 protein) is represented with green (starting structure) and purple (final structure) ribbons respectively. Chain A (C8 indel peptide) is represented with cyan (starting structure) and orange (final structure) ribbons respectively. **B**) Bundle of ten indel peptide structures, superimposed over heavy atoms. One frame every 1.5 ns were obtained. Structures were fitted with RMSD slightly less than 0.06 nm. Reproduced after permission from Springer, J Mol Mod (2009) 15:165-171 (For interpretation of the references to color in this figure legend, the reader is referred to the web version of this paper).

Ray structure, both Ala_{164} and Ala_{40} residues of C8α and C8γ chains respectively were replaced with cysteine residues and a disulfide bond was imposed between them. The heterodimer complex was subjected to molecular dynamics simulation in explicit water in order to extract the dynamical properties of association and to examine the stability of the proposed disulfide bonded complex. Results revealed that the heterodimeric complex is stable, under MD conditions, and supported the association hypothesis. Moreover, Slade *et al.* published [128] the crystal structure of the C8γ/C8α complex (Fig. **6**). These crystallographic data corroborated the association hypothesis and provided a validation framework of the MD study and the proposed model.

CONCLUSIONS

The applications of MD simulations in the area of peptide vaccine design have been highlighted in this review. The main areas of focus of the simulations are: molecular modeling of new targets and mutants and binding energetics of immunogenic peptides to their cognate receptors. Despite being crude approximation of the actual forces in a molecular system, force fields used by MD software can give a good estimate of the molecular forces that govern the dynamics of a system. And it is this dynamic behavior of the biological systems that can not be neglected in modern computer-aided drug design.

In general three main areas of interest in applying MD simulations in immunological complexes can be specified:

1. simulation of an x-ray structure to explore structural and energetic features of the binding process
2. simulation of a mutated protein or complex to explore the impact of the mutation to the complex formation
3. simulation of modeled structure, usually after homology modeling of docking

In all these three general cases, MD simulations have offered a unique insight into structure and function of immunological proteins and their complexes. It is expected these theoretical techniques will be applied more widely and to more sophisticated systems will be studied. The appearance of patient-specific simulation in AIDS treatment [25] leaves a lot of promises to other areas in clinical research related with immunology.

Recent advances in supercomputer power have allowed the utilization of MD simulations towards computation of free energy of binding of big systems such as TCR/peptide/MHC complexes [25, 71]. While detailed coverage of this topic is not within the purposes of this review, it must be underlined that the significance of this approach is rather high. Computing thermodynamic values from MD simulations that are directly comparable with experimentally obtained values should bring theoreticians and experimentalists more close [15] in searching for new drugs. It is expected that these techniques will be applied extensively in the future and that they would contribute substantially to the scientific effort for better understanding

the immune system and producing more effective drugs and vaccines.

AKNOWLEDGEMENTS

The author thanks two anonymous referees for constructive and fruitful comments.

ABBREVIATIONS

ABF	=	Adaptive biasing force
AChR	=	Nicotinic acetylcholine receptor
APL	=	Altered peptide ligands
AS	=	Ankylosing spondylitis
BPTI	=	Bovine Protein Trypsin Inhibitor
BSA	=	Buried surface area
CTL	=	Cytotoxic T lymphocytes
FEP	=	Free energy pertubation
HLA	=	Human leukocyte antigen
HRS	=	Histidyl-tRNA synthetase
MBP	=	Myelin basic protein
MD	=	Molecular dynamics
MHC	=	Major histocompatibility complex
MIR	=	Main immunogenic region
MM-PBSA	=	Molecular mechanics Poisson-Boltzmann surface area
NMR	=	Nuclear magnetic resonance
PDB	=	Protein data bank
PSF	=	Protein structure file
RMSD	=	Root mean square deviation
RMSF	=	Root mean square fluctuation
TI	=	Thermodynamic integration
TCR	=	T cell receptor

REFERENCES

[1] Loffet, A. Peptides as drugs: is there a market? *J. Pept. Sci.*, **2002**, *8*, 1-7.

[2] Otvos, L.J. Peptide-based drug design: here and now. *Methods Mol. Biol.*, **2008**, *494*, 1-8.

[3] Dings, R.P.; Mayo, K.H. A journey in structure-based drug discovery: from designed peptides to protein surface topomimetics as antibiotic and antiangiogenic agents. *Acc. Chem. Res.*, **2007**, *40*, 1057-1065.

[4] Clynen, E.; Baggerman, G.; Husson, S.J.; Landuyt, B.; Schoofs, L. Peptidomics in drug research. *Exp. Opin. Drug Disc.*, **2008**, *3*, 425-440.

[5] Stavrakoudis, A. Conformational studies of the 313-320 and 313-332 peptide fragments derived from the αIIb subunit of integrin receptor with molecular dynamics simulations. *Int. J. Pept. Res. Ther.*, **2009**, *15*, 263-272.

[6] Andrusier, N.; Mashiach, E.; Nussinov, R.; Wolfson, H.J. Principles of flexible protein-protein docking. *Proteins*, **2008**, *73*, 271-289.

[7] Alberts, I.L.; Todorov, N.P.; Dean, P.M. Receptor flexibility in *de novo* ligand design and docking. *J. Med. Chem.*, **2005**, *48*, 6585-6596.

[8] Carlson, H.A.; McCammon, J.A. Accommodating protein flexibility in computational drug design. *Mol. Pharmacol.*, **2000**, *57*, 213-218.

[9] Brooijmans, N.; Kuntz, I.D. Molecular recognition and docking algorithms. *Annu. Rev. Biophys. Biomol. Struct.*, **2003**, *32*, 335-373.

[10] B-Rao, C.; Subramanian, J.; Sharma, S.D. Managing protein flexibility in docking and its applications. *Drug Discov. Today*, **2009**, *14*, 394-400.

[11] Legge, F.S.; Budi, A.; Treutlein, H.; Yarovsky, I. Protein flexibility: multiple molecular dynamics simulations of insulin chain B. *Biophys. Chem.*, **2006**, *119*, 146-157.

[12] Jorgensen, W.L. The many roles of computation in drug discovery. *Science*, **2004**, *303*, 1813-1318.

[13] Galeazzi, R. Molecular dynamics as a tool in rational drug design: current status and some major applications. *Curr. Comput.-Aided Drug Des.*, **2009**, *5*, 225-240.

[14] McCammon, J.A.; Gelin, B.R.; Karplus, M. Dynamics of folded proteins. *Nature*, **1977**, *267*, 585-590.

[15] van Gunsteren, W.F.; Dolenc, J.; Mark, A.E. Molecular simulation as an aid to experimentalists. *Curr. Opin. Struct. Biol.*, **2008**, *18*, 149-153.

[16] Karplus, M.; McCammon, J.A. Molecular Dynamics simulations of biomolecules. *Nat. Struct. Biol.*, **2002**, *9*, 646-652.

[17] Mackerell, A.D.J.; Feig, M.; Feig, M.F.; Brooks, C.L. 3rd Extending the treatment of backbone energetics in protein force fields: limitations of gas-phase quantum mechanics in reproducing protein conformational distributions in molecular dynamics simulations. *J. Comput. Chem.*, **2004**, *25*, 1400-1415.

[18] Stavrakoudis, A. Molecular dynamics simulations of an apoliprotein A-I derived peptide in explicit water. *Chem. Phys. Lett.*, **2008**, *461*, 294-299.

[19] Ponder, J.W.; Case, D.A. Force fields for protein simulations. *Adv. Protein Chem.*, **2003**, *66*, 27-85.

[20] MacKerell, A.D.J. Empirical force fields for biological macromolecules: overview and issues. *J. Comput. Chem.*, **2004**, *25*, 1584-1604.

[21] van Gunsteren, W.F.; Balkowies, D.; Baron, R.; Chandrasekhar, I.; Christen, M.; Daura, X.; Gee, P.; Geerke, D.P.; Glattli, A.; Hunenberger, P.H.; Kastenholz, M.A.; Oostenbrink, C.; Schenk, M.; Trzesniak, D.; van der Vegt, N.F.A.; Yu, B.Y. Biomolecular modeling: goals, problems, perspectives. *Angew Chem. Int. Ed. Engl.*, **2006**, *45*, 4064-4092.

[22] Flower, D.R. Towards *in silico* prediction of immunogenic epitopes. *Trends Immunol.*, **2003**, *24*, 667-674

[23] Saksena, R.S.; Boghosian, B.; Fazendeiro, L.; Kenway, O.A.; Manos, S.; Mazzeo, M.D.; Sadiq, S.K.; Suter, J.L.; Wright, D.; Coveney, P.V. Real science at the petascale. *Philos. Transact. A Math Phys. Eng. Sci.*, **2009**, *367*, 2557-2571.

[24] Sadiq, S.K.; Wright, D.; Watson, S.J.; Zasada, S.J.; Stoica, I.; Coveney, P.V. Automated molecular simulation based binding affinity calculator for ligand-bound HIV-1 proteases. *J. Chem. Inf. Model.*, **2008**, *48*, 1909-1919.

[25] Sadiq, S.K.; Mazzeo, M.D.; Zasada, S.J.; Manos, S.; Stoica, I.; Gale, C.V.; Watson, S.J.; Kellam, P.; Brew, S.; Coveney, P.V. Patient-specific simulation as a basis for clinical decision-making. *Philos. Transact. A Math Phys. Eng. Sci.*, **2008**, *366*, 3199-3219.

[26] Mallik, B.; Morikis, D. Applications of molecular dynamics simulations in immunology: a useful computational method in aiding vaccine design. *Curr. Proteomics*, **2006**, *3*, 259-270.

[27] Rognan, D.; Reddehase, M.J.; Koszinowski, U.H.; Folkers, G. Molecular modeling of an antigenic complex between a viral peptide and a class I major histocompatibility glycoprotein. *Proteins*, **1992**, *13*, 70-85.

[28] Stavrakoudis, A.; Demetropoulos, I.N.; Sakarellos, C.; Sakarellos-Daitsiotis, M.; Tsikaris, V. Design, synthesis and catalytic activity of a serine protease synthetic model. *Int. J. Pept. Res. Ther.*, **1997**, *4*, 481-487.

[29] Stavrakoudis, A.; Makropoulou, S.; Tsikaris, V.; Sakarellos-Daitsiotis, M.; Sakarellos, C.; Demetropoulos, I.N. Computational screening of branched cyclic peptide motifs as potential enzyme mimetics. *J. Pept. Sci.*, **2003**, *9*, 145-155.

[30] Tatsis, V.A.; Stavrakoudis, A.; Demetropoulos, I.N. LysinebasedTrypsinActSite(LysTAS): A configurational tool of the TINKER software to evaluate Lysine based branched cyclic

peptides as potential chymotrypsin-mimetics. *Mol. Simul.*, **2006**, *32*, 643-644.

[31] Tatsis, V.A.; Stavrakoudis, A.; Demetropoulos, I.N. Molecular Dynamics as a pattern recognition tool: An automated process detects peptides that preserve the 3D arrangement of trypsin's active site. *Biophys. Chem.*, **2008**, *133*, 36-44.

[32] Stavrakoudis, A.; Tsoulos, I.G.; Shenkarev, Z.O.; Ovchinnikova, T.V. Molecular dynamics simulation of antimicrobial peptide arenicin-2: beta-hairpin stabilization by noncovalent interactions. *Biopolymers*, **2009**, *92*, 143-155.

[33] Mehrnejad, F.; Naderi-Manesh, H.; Ranjbar, B. The structural properties of magainin in water, TFE/water, and aqueous urea solutions: molecular dynamics simulations. *Proteins*, **2007**, *67*, 931-940.

[34] Trzesniak, D.; Glattli, A.; Jaun, B.; van Gunsteren, W.F. Interpreting NMR data for beta-peptides using molecular dynamics simulations. *J. Am. Chem. Soc.*, **2005**, *127*, 14320-14329.

[35] Sorin, E.J.; Pande, V.S. Exploring the helix-coil transition *via* all-atom equilibrium ensemble simulations. *Biophys. J.*, **2005**, *88*, 2472-2493.

[36] Duan, Y.; Kollman, P.A. Pathways to a protein folding intermediate observed in a 1-microsecond simulation in aqueous solution. *Science*, **1998**, *282*, 740-744.

[37] Cornell, W.D.; Cieplak, P.; Bayly, C.I.; Gould, I.R.; Merz, K.M.; Ferguson, D.M.; Spellmeyer, D.C.; Fox, T.; Caldwell, J.W.; Kollman, P.A. A second generation force field for the simulation of proteins, nucleic acids, and organic molecules. *J. Am. Chem. Soc.*, **1996**, *118*, 2309–2309.

[38] Brooks, B.R.; Bruccoleri, R.E.; Olafson, B.D.; States, D.J.; Swaminathan, S.; Karplus, M. CHARMM-A program for macromolecular energy, minimization, and dynamics calculations. *J. Comput. Chem.*, **1983**, *4*, 187-217.

[39] Phillips, J.C.; Braun, R.; Wang, W.; Gumbart, J.; Tajkhorshid, E.; Villa, E.; Chipot, C.; Skeel, R.D.; Kale, L.; Schulten, K. Scalable molecular dynamics with NAMD. *J. Comput. Chem.*, **2005**, *26*, 1781-1802.

[40] Scott, W.R.P.; Hunenberger, P.H.; Tironi, I.G.; Mark, A.E.; Billeter, S.R.; Fennen, J.; Torda, A.E.; Huber, T.; Kruger, P.; van Gunsteren, W.F. The GROMOS biomolecular simulation program package. *J. Phys. Chem. A*, **1999**, *103*, 3596–3607.

[41] Berendsen, H.J.C.; van der Spoel, D.; van Drunen, R. GROMACS: A message-passing parallel molecular dynamics implementation. *Comput. Phys. Commun.*, **1995**, *91*, 43-56.

[42] Glykos, N.M. Carma: a molecular dynamics analysis program. *J. Comput. Chem.*, **2006**, *27*, 1765-1768.

[43] Garrant, B.; McCammon, J.A. Bio3D: analysis. *Bioinformatics*, **2006**, *11*, 11-21.

[44] Grochowski, P.; Trylska, J. Continuum molecular electrostatics, salt effects, and counterion binding - a review of the Poisson-Boltzmann theory and its modifications. *Biopolymers*, **2008**, *89*, 93-113.

[45] Bashford, D.; Case, D.A. Generalized born models of macromolecular solvation effects. *Annu. Rev. Phys. Chem.*, **2000**, *51*, 129-152.

[46] Roux, B.; Simonson, T. Implicit solvent models. *Biophys. Chem.*, **1999**, *78*, 1-20.

[47] Gilson, M.K.; Zhou, H.X. Calculation of protein-ligand binding affinities. *Annu. Rev. Biophys. Biomol. Struct.*, **2007**, *36*, 21-42.

[48] Sitkoff, D.; Sharp, K.A.; Honig, B. Accurate calculation of hydration free-energies using macroscopic solvent models. *J. Phys. Chem.*, **1994**, *98*, 1978-1988.

[49] Massova, I.; Kollman, P.A. Computational alanine scanning to probe protein–protein interactions: a novel approach to evaluate binding free energies. *J. Am. Chem. Soc.*, **1999**, *121*, 8133-8143.

[50] Simonson, T.; Archontis, G.; Karplus, M. Free energy simulations come of age: protein-ligand recognition. *Acc. Chem. Res.*, **2002**, *35*, 430-437.

[51] Kuhn, B.; Gerber, P.; Schulz-Gasch, T.; Stahl, M. Validation and use of the MM-PBSA approach for drug discovery. *J. Med. Chem.*, **2005**, *48*, 4040–4048.

[52] Swanson, J.M.J.; Henchman, R.H.; McCammon, J.A. Revisiting free energy calculations: a theoretical connection to MM/PBSA and direct calculations of the association free energy. *Biophys. J.*, **2004**, *86*, 67-74.

[53] Fogolari, F.; Brigo, A.; Molinari, H. Protocol for MM/PBSA molecular dynamics simulations of proteins. *Biophys. J.*, **2003**, *85*, 159-166.

[54] Ooi, T.; Oobatake, M.; Nemethy, G.; Scheraga, H.A. Accessible surface areas as a measure of the thermodynamic parameters of hydration of peptides. *Proc. Natl. Acad. Sci. USA*, **1987**, *84*, 3086-3090.

[55] Baker, N.A.; Sept, D.; Joseph, S.; Holst, M.J.; McCammon, J.A. Electrostatics of nanosystems: application to microtubules and the ribosome. *Proc. Natl. Acad. Sci. USA*, **2001**, *98*, 10037-10041.

[56] Brooks, B.R.; Janesic, D.; Karplus, M. Harmonic analysis of large systems. I. methodology. *J. Comput. Chem.*, **1995**, *16*, 1522-1542.

[57] Carlsson, J.; Aqvist, J. Calculations of solute and solvent entropies from molecular dynamics simulations. *Phys. Chem. Chem. Phys.*, **2006**, *8*, 5385-5395.

[58] Karplus, M.; Kushick, J.N. Method for estimating the configurational entropy of macromolecules. *Macromolecules*, **1981**, *14*, 325-332.

[59] Killian, B.J.; Kravitz, J.Y.; Somani, S.; Dasgupta, P.; Pang, Y.-P.; Gilson, M.K. Configurational entropy in protein–peptide binding: computational study of Tsg101 ubiquitin E2 variant domain with an hiv-derived PTAP nonapeptide. *J. Mol. Biol.*, **2009**, *389*, 315-335.

[60] Hsu, S.-T.D.; Peter, C.; van Gunsteren, W.F.; Bonvin, M.J.J. Entropy calculation of HIV-1 Env gp120, its receptor CD4, and their complex: an analysis of configurational entropy changes upon complexation. *Biophys. J.*, **2005**, *88*, 15-24.

[61] Schlitter, J. Estimation of absolute and relative entropies of macromolecules using the covariance-matrix. *Chem. Phys. Lett.*, **1993**, *215*, 487-496.

[62] Grossfield, A.; Feller, S.E.; Pitman, M.C. Convergence of molecular dynamics simulations of membrane proteins. *Proteins*, **2007**, *67*, 31-40.

[63] Smith, B.J.; Daura, X.; Van Gunsteren, W.F. Assessing equilibration and convergence in biomolecular simulations. *Proteins: Struct. Funct. Bioinf.*, **2002**, *48*, 487-496.

[64] Yang, W.; Bitetti-Putzer, R.; Karplus, M. Free energy simulations: use of reverse cumulative averaging to determine the equilibrated region and the time required for convergence. *J. Chem. Phys.*, **2004**, *120*, 2618-2628.

[65] Lyman, E.; Zuckerman, D.M. Ensemble-based convergence analysis of biomolecular trajectories. *Biophys. J.*, **2006**, *91*, 164-172.

[66] Pappalardo, F.; Halling-Brown, M.D.; Rapin, N.; Zhang, P.; Alemani, D.; Emerson, A.; Paci, P.; Duroux, P.; Pennisi, M.; Palladini, A.; Miotto, O.; Churchill, D.; Rossi, E.; Shepherd, A.J.; Moss, D.S.; Castiglione, F.; Bernaschi, M.; Lefranc, M.P.; Brunak, S.; Motta, S.; Lollini, P.L.; Basford, K.E.; Brusic, V. ImmunoGrid, an integrative environment for large-scale simulation of the immune system for vaccine discovery, design and optimization. *Brief Bioinform.*, **2009**, *10*, 330-340.

[67] Zhang, G.L.; Khan, A.M.; Srinivasan, K.N.; August, J.T.; Brusic, V. MULTIPRED: a computational system for prediction of promiscuous HLA binding peptides. *Nucleic Acids Res.*, **2005**, *33*, W172-179.

[68] Tong, J.C.; Ren, E.C. Immunoinformatics: Current trends and future directions. *Drug Discov. Today*, **2009**, *14*, 684-689.

[69] Todman, S.J.; Halling-Brown, M.D.; Davies, M.N.; Flower, D.R.; Kayikci, M.; Moss, D.S. Toward the atomistic simulation of T cell epitopes automated construction of MHC: peptide structures for free energy calculations. *J. Mol. Graph. Model.*, **2008**, *26*, 957-961.

[70] Schafroth, D.H.; Floudas, A.C. Predicting peptide binding to MHC pockets *via* molecular modeling, implicit solvation, and global optimization. *Proteins: Struct. Funct. Bioinf.*, **2004**, *54*, 534 - 556.

[71] Wan, S.; Flower, D.R.; Coveney, P.V. Toward an atomistic understanding of the immune synapse: Large-scale molecular dynamics simulation of a membrane-embedded TCR-pMHC-CD4 complex. *Mol. Immunol.*, **2008**, *45*, 1221-1230.

[72] Sieker, F.; May, A.; Zacharias, M. Predicting affinity and specificity of antigenic Peptide binding to major histocompatibility class I molecules. *Curr. Protein Pept. Sci.*, **2009**, *10*, 286-296.

[73] Petrone, P.M.; Garcia, A.E. MHC-peptide binding is assisted by bound water molecules. *J. Mol. Biol.*, **2004**, *338*, 419-435.

[74] Knapp, B.; Omasits, U.; Bohle, B.; Maillere, B.; Ebner, C.; Schreiner, W.; Jahn-Schmid, B. 3-Layer-based analysis of peptide-MHC interaction: *in silico* prediction, peptide binding affinity and

T cell activation in a relevant allergen-specific model. *Mol. Immunol.*, **2009**, *46*, 1839-1844.

[75] Fagerberg, T.; Cerottini, J.C.; Michielin, O. Structural prediction of peptides bound to MHC class I. *J. Mol. Biol.*, **2006**, *356*, 521-546.

[76] Rognan, D.; Zimmermann, N.; Jung, G.; Gerd Folkers, G. Molecular dynamics study of a complex between the human histocompatibility antigen HLA-A2 and the IMP58-66 nonapeptide from influenza virus matrix protein. *Eur. J. Biochem.*, **1992**, *208*, 101–113.

[77] Madden, D.R.; Gorga, J.C.; Strominger, J.L.; Wiley, D.C. The three-dimensional structure of HLA-B27 at 2.1 A resolution suggests a general mechanism for tight peptide binding to MHC. *Cell*, **1992**, *70*, 1035-1048.

[78] Toh, H.; Savoie, C.S.; Kamikawaji, N.; Muta, S.; Sasazuki, T.; Kuhara, S. Changes at the floor of the peptide-binding groove induce a strong preference for proline at position 3 of the bound peptide: Molecular dynamics simulations of HLA-A*0217. *Biopolymers*, **2000**, *54*, 318 - 327.

[79] Joseph, M.A.; Mitchell, M.L.; Evanseck, J.D.; Kovacs, J.R.; Jia, L.; Shen, H.; Meng, W.S. Secondary anchor substitutions in an HLA-A*0201-restricted T-cell epitope derived from Her-2/neu. *Mol. Immunol.*, **2007**, *44*, 322-331.

[80] Kuhns, J.J.; Batalia, M.A.; Yan, S.; Collins, E.J. Poor binding of a HER-2/neu epitope (GP2) to HLA-A2.1 is due to a lack of interactions with the center of the peptide. *J. Biol. Chem.*, **1999**, *274*, 36422-36427.

[81] Meng, W.S.; von Grafenstein, H.; Haworth, I.S. Water dynamics at the binding interface of four different HLA-A2-peptide complexes. *Int. Immunol.*, **2000**, *12*, 949-957.

[82] Ma, B.; Nussinov, R. Trp/Met/Phe hot spots in protein-protein interactions: potential targets in drug design. *Curr. Top. Med. Chem.*, **2007**, *7*, 999-1005.

[83] Fiorillo, M.T.; Maragno, M.; Butler, R.; Dupuis, M.L.; Sorrentino, R. CD8(+) T-cell autoreactivity to an HLA-B27 restricted self-epitope correlates with ankylosing spondylytis. *J. Clin. Invest.*, **2000**, *106*, 47-53.

[84] Hülsmeyer, M.; Fiorillo, M.T.; Bettosini, F.; Sorrentino, R.; Saenger, W.; Ziegler, A.; Uchanska-Ziegler, B. Dual, HLA-B27 subtype-dependent conformation of a self-peptide. *J. Exp. Med.*, **2004**, *199*, 271-281.

[85] Fabian, H.; Huser, H.; Narzi, D.; Misselwitz, R.; Loll, B.; Ziegler, A.; Bockmann, R.A.; Uchanska-Ziegler, B.; Naumann, D. HLA-B27 subtypes differentially associated with disease exhibit conformational differences in solution. *J. Mol. Biol.*, **2008**, *376*, 798-810.

[86] Lazoura, E.; Lodding, J.; Farrugia, W.; Ramsland, P.A.; Apostolopoulos, V. Non-canonical anchor motif peptides bound to MHC class I induce cellular responses. *Mol. Immunol.*, **2009**, *46*, 1171-1178.

[87] Toh, H.; Kamikawaji, N.; Tana, T.; Sasazuki, T.; Kuhara, S. Molecular dynamics simulations of HLA-DR4 (DRB1*0405) complexed with analogue peptide: conformational changes in the putative T-cell receptor binding regions. *Protein Eng.*, **1998**, *11*, 1027-1032.

[88] Zavala-Ruiz, Z.; Strug, I.; Walker, B.D.; Norris, P.J.; Stern, L.J. A hairpin turn in a class II MHC-bound peptide orients residues outside the binding groove for T cell recognition. *Proc. Natl. Acad. Sci. USA*, **2004**, *101*, 13279-13284.

[89] Mantzourani, E.D.; Platts, J.A.; Brancale, A.; Mavromoustakos, T.M.; Tselios, T.V. Molecular dynamics at the receptor level of immunodominant myelin basic protein epitope 87-99 implicated in multiple sclerosis and its antagonists altered peptide ligands: triggering of immune response. *J. Mol. Graph. Model.*, **2007**, *26*, 471-481.

[90] Li, Z.; Lazaridis, T. Water at biomolecular binding interfaces. *Phys. Chem. Chem. Phys.*, **2007**, *9*, 573-580.

[91] Wong, S.; Amaro, R.E.; McCammon, J.A. MM-PBSA captures key role of intercalating water molecules at a protein-protein interface. *J. Chem. Theory Comput.*, **2009**, *5*, 422-429.

[92] Painter, C.A.; Cruz, A.; Lopez, G.E.; Stern, L.J.; Zavala-Ruiz, Z. Model for the peptide-free conformation of class II MHC proteins. *PLoS Biol.*, **2008**, *3*, e2403.

[93] Villa, E.; Balaeff, A.; Schulten, K. Structural dynamics of the lac repressor-DNA complex revealed by a multiscale simulation. *Proc. Natl. Acad. Sci. USA*, **2005**, *102*, 6783–6788.

[94] Zacharias, M.; Springer, S. Conformational flexibility of the MHC class I alpha1-alpha2 domain in peptide bound and free states: a molecular dynamics simulation study. *Biophys. J.*, **2004**, *87*, 2203-2214.

[95] Sundberg, E.J.; Mariuzza, R.A. Molecular recognition in antibody-antigen complexes. *Adv. Protein Chem.*, **2002**, *61*, 119-160.

[96] MacCallum, R.M.; Martin, A.C.; Thornton, J.M. Antibody-antigen interactions: contact analysis and binding site topography. *J. Mol. Biol.*, **1996**, *262*, 732-745.

[97] Lafont, V.; Schaefer, M.; Stote, R.H.; Altschuh, D.; Dejaegere, A. Protein-protein recognition and interaction hot spots in an antigen-antibody complex: free energy decomposition identifies "efficient amino acids". *Proteins: Struct. Funct. Bioinf.*, **2007**, *67*, 418-434.

[98] Oomen, C.J.; Hoogerhout, P.; Bonvin, A.M.; Kuipers, B.; Brugghe, H.; Timmermans, H.; Haseley, S.R.; van Alphen, L.; Gros, P. Immunogenicity of peptide-vaccine candidates predicted by molecular dynamics simulations. *J. Mol. Biol.*, **2003**, *328*, 1083-1089.

[99] Lapelosa, M.; Gallicchio, E.; Arnold, G.F.; Arnold, E.; Levy, R.M. *In silico* vaccine design based on molecular simulations of rhinovirus chimeras presenting HIV-1 gp41 epitopes. *J. Mol. Biol.*, **2009**, *385*, 675-691.

[100] Lorenzo, B.; Duccio, F.; Francesco, P.; Paolo De Los, R.; Michel, S.; Ulf, S. A dynamical study of antibody-antigen encounter reactions. *Phys. Biol.*, **2007**, *4*, 172-180.

[101] Orlewski, P.; Marraud, M.; Cung, M.T.; Tsikaris, V.; Sakarellos-Daitsiotis, M.; Sakarellos, C.; Vatzaki, E.; Tzartos, S.J. Compared structures of the free nicotinic acetylcholine receptor main immunogenic region (MIR) decapeptide and the antibody-bound [A76]MIR analogue: a molecular dynamics simulation from two-dimensional NMR data. *Biopolymers*, **1996**, *40*, 419-432.

[102] Tsikaris, V.; Detsikas, E.; Sakarellos-Daitsiotis, M.; Sakarellos, C.; Vatzaki, E.; Tzartos, S.J.; Marraud, M.; Cung, M.T. Conformational requirements for molecular recognition of acetylcholine receptor main immunogenic region (MIR) analogues by monoclonal anti-MIR antibody: a two-dimensional nuclear magnetic resonance and molecular dynamics approach. *Biopolymers*, **1993**, *33*, 1123-1134.

[103] Kleinjung, J.; Petit, M.-C.; Orlewski, P.; Mamalaki, A.; Tzartos, S.J.; Tsikaris, V.; Sakarellos-Daitsiotis, M.; Sakarellos, C.; Marraud, M.; Cung, M.-T. The third-dimensional structure of the complex between an Fv antibody fragment and an analogue of the main immunogenic region of the acetylcholine receptor: a combined two-dimensional NMR, homology, and molecular modeling approach. *Biopolymers*, **2000**, *53*, 113-128.

[104] Wilson, I.A. Antibody-antigen interactions: new structures and new conformational changes. *Curr. Opin. Struct. Biol.*, **1994**, *4*, 857-867.

[105] van Regenmortel, M.H. Antigenicity and immunogenicity of synthetic peptides. *Biologicals*, **2001**, *29*, 209-213.

[106] Mahler, M.; Bluthner, M.; Pollard, K.M. Advances in B-cell epitope analysis of autoantigens in connective tissue diseases. *Clin. Immunol.*, **2003**, *107*, 65-79.

[107] Camacho, C.J.; Katsumata, Y.; Ascherman, D.P. Structural and thermodynamic approach to peptide immunogenicity. *PLoS Comput. Biol.*, **2008**, *4*, e100231.

[108] van der Ley, P.; Heckels, J.; Virji, M.; Hoogerhout, P.; Pollman, J.T. Topology of outer membrane porins in pathogenic *Neisseria*. *Infect. Immun.*, **1991**, *59*, 2963-2971.

[109] van der Elsen, J.; Herron, J.N.; Hoogerhout, P.; Pollman, J.T.; Boel, E.; Logtenberg, T. Bactericidal antibody recognition of a PorA epitope of *Neisseria meningitis*: crystal structure of a Fab fragment in complex with a fluerescein-conjugated peptide. *Proteins: Struct. Funct. Genet.*, **1997**, *29*, 113-125.

[110] Ramirez-Alvarado, M.; Blanco, F.J.; Niemann, H.; Serrano, L. Role of the beta-turn residues in the beta-hairpin formaton and stability in designed pepides. *J. Mol. Biol.*, **1997**, *273*, 898-912.

[111] Ramirez-Alvarado, M.; Kortemme, T.; Blanco, F.J.; Serrano, L. Beta-hairpin and beta-sheet formation in designed linear peptides. *Bioorg. Med. Chem.*, **1999**, *7*, 93-103.

[112] Christodoulides, M.; McGuiness, B.T.; Heckels, J.E. immunization with synthetic peptides containing epitopes of the class 1 outer-membrane protein of Neisseria meningitis: production of bactericidal antibodies on immunization with a cyclic peptide. *J. Gen. Microbiol.*, **1993**, *139*, 1729-1738.

[113] Kee, K.S.; Jois, S.D. Design of beta-turn based therapeutic agents. *Curr. Pharm. Des.*, **2003**, *9*, 1209-1224.
[114] Oomen, C.J.; Hoogerhout, P.; Kuipers, B.; Vidarsson, G.; Van Alphen, L.; Gros, P. Crystal structure of an anti-meningococcal subtype P1.4 PorA antibody provides basis for peptide-vaccine design. *J. Mol. Biol.*, **2005**, *351*, 1070-1080.
[115] Almagro, J.C.; Fransson, J. Humanization of antibodies. *Front. Biosci.*, **2008**, *13*, 1619-1633.
[116] Domagala, A.; Kurpisz, M. CD52 antigen - a review. *Med. Sci. Monit.*, **2001**, *7*, 325-331.
[117] Schmouder, R.L. Immunosuppressive therapies for the twenty-first century. *Transpl. Proc.*, **2000**, *32*, 1463-1467.
[118] Dumont, F.J. CAMPATH (alemtuzumab) for the treatment of chronic lymphocytic leukemia and beyond. *Exp. Rev. Anticancer Ther.*, **2002**, *2*, 23-35.
[119] James, L.C.; Hale, G.; Waldmann, H.; Bloomer, A.C. 1.9 A structure of the therapeutic antibody CAMPATH-1H fab in complex with a synthetic peptide antigen. *J. Mol. Biol.*, **1999**, *289*, 293-301.
[120] Tatsis, V.A.; Tsoulos, I.G.; Stavrakoudis, A. Molecular dynamics simulations of the TSSPSAD peptide antigen in free and bound with CAMPATH-1H Fab antibody states: the importance of the β-turn conformation. *Int. J. Pept. Res. Ther.*, **2009**, *15*, 1-7.
[121] Stavrakoudis, A. Computational modelling and molecular dynamics simulations of a cycliccpeptide mimotope of the CD52 antigen complexed with CAMPATH-1H antibody. *Mol. Simul.*, **2010**, *26*, 127-137.
[122] Zhang, L.; Mallik, B.; Morikis, D. Immunophysical exploration of C3d–CR2(CCP1-2) interaction using molecular dynamics and electrostatics. *J. Mol. Biol.*, **2007**, *369*, 567-583.
[123] Haspel, N.; Ricklin, D.; Geisbrecht, B.V.; Kavraki, L.E.; Lambris, J.D. Electrostatic contributions drive the interaction between Staphylococcus aureus protein Efb-C and its complement target C3d. *Protein Sci.*, **2008**, *16*, 1894-1906.
[124] Ng, S.C.; Gururaj Rao, A.; Zack Howard, O.M.; Sodetz, J.M. The eighth component of human complement: Evidence that it is an oligomeric serum protein assembled from products of three different genes. *Biochemistry*, **1987**, *26*, 5229-5233.
[125] Plumb, M.E.; Sodetz, J.M. An indel within the C8 alpha subunit of human complement C8 mediates intracellular binding of C8 gamma and formation of C8 alpha-gamma. *Biochemistry*, **2000**, *39*, 13078-13083.
[126] Lovelace, L.L.; Chiswell, B.; Slade, D.J.; Sodetz, J.M.; Lebioda, L. Crystal structure of complement protein C8gamma in complex with a peptide containing the C8gamma binding site on C8alpha: implications for C8gamma ligand binding. *Mol. Immunol.*, **2008**, *45*, 750-756.
[127] Stavrakoudis, A. A disulfide linked model of the complement protein C8γ complexed with C8α indel peptide. *J. Mol. Model.*, **2009**, *15*, 165-171.
[128] Slade, D.J.; Lovelace, L.L.; Chruszcz, M.; Minor, W.; Lebioda, L.; Sodetz, J.M. Crystal structure of the MACPF domain of human complement protein C8alpha in complex with the C8gamma subunit. *J. Mol Biol.*, **2008**, *379*, 331-342.

Received: January 15, 2010 **Revised: March 10, 2010** **Accepted: April 15, 2010**